A simple model of plate-like crystallization with constant plate thickness

Beata Misztal-Faraj[a)]
Polymer Physics Department, Institute of Fundamental Technological Research, Polish Academy of Sciences, 02-106 Warsaw, Poland

(Received 6 August 2012; accepted 18 March 2013)

A kinetic model of crystallization based on two-dimensional nucleation and growth of plate-like crystals with constant thickness is analyzed. It is shown that plate thickness required for nucleation is limited. The lower limit is determined by zero Gibbs' free energy of transition, the upper one corresponds to the conditions when the critical cluster volume of nucleation is equal to two elementary kinetic units. Effects of plate thickness on crystallization kinetics are discussed. In the lower temperature range, creation of thicker plates is preferred. For a given plate thickness, frequency of the phase transition decreases with increasing temperature. Numerical calculations for α-polypropylene concern kinetics of primary nucleation and global phase transition in a system of one or several fractions of plate-like kinetic elements.

I. INTRODUCTION

Physical properties of materials strongly depend on their internal structure and indirectly on formation conditions. Modeling of processes of structure development allows to predict and control structures obtained under different conditions and to optimize material properties.

In the recent two papers,[1,2] influence of crystallization conditions on the content of polymorphic phases and on the kinetics of polymorphic crystallization was discussed. α and β polymorphs of isotactic polypropylene were taken as an example. The probabilistic theory of Kolmogorov,[3] Avrami,[4–6] and Evans[7] was used, in which particles of the amorphous phase aggregate to form crystal nuclei and subsequently grow in three dimensions (Fig. 1). For the sake of simplicity, the aggregating kinetic units are assumed as cubes.

The model calculations for isothermal crystallization were qualitatively consistent with experimental data on polypropylene.[8]

In the present paper, another model is analyzed, one involving anisotropic tetragonal units aggregating into two-dimensional plate-like crystal nuclei (Fig. 2).

The idea of plate-like crystallization of polymers was introduced by Keller,[9] Hoffman, Lauritzen, and others[10–12] who described morphology of polymer crystallization in terms of folded polymer chains. The Hoffman–Lauritzen treatment was concentrated on plate growth and the overall crystallization kinetics was not analyzed. A complete kinetic model of plate-like crystallization, consisting of primary nucleation and crystal growth, will be presented. The model will admit distribution of plate thickness, which may account for distributed melting. It is assumed that each fraction of plates is created from a different precursor with a given plate thickness. This characteristic does not change in the process of crystallization. It is also assumed that polymorphic transitions between different plate-like phases are not allowed for kinetic reasons.

The plate-like model may be useful for describing crystallization of liquids consisting of rigid anisotropic molecules as well as crystallization of polymers with folded chains.

The aim of this work is to analyze effects of crystallization conditions on nucleation and growth of plate-like crystals. The results are illustrated with example calculations. The limits of nucleation-controlled crystallization are also discussed.

The model is shown to reproduce reasonably well temperature behavior of plate thickness for linear polyethylene and isothermal crystallization rate of α-polypropylene.

II. FUNDAMENTAL EQUATIONS OF THE MODEL

A. Thermodynamics

1. Ideal liquid-melt system

The phase diagram of an ideal two-phase crystalline-amorphous system is presented in Fig. 3.

The two phases—liquid (amorphous) phase "0" and solid phase "∞"—are of infinite size. Both phases are thermodynamically stable and their coexistence is determined by a single equilibrium melting temperature, $T_{\infty 0}$.

For the sake of simplicity, linear dependence of the Gibbs' free energy on temperature is assumed as follows:

a)Address all correspondence to this author.
e-mail: bfaraj@ippt.gov.pl
DOI: 10.1557/jmr.2013.74

 © Materials Research Society 2013

https://doi.org/10.1557/jmr.2013.74 Published online by Cambridge University Press

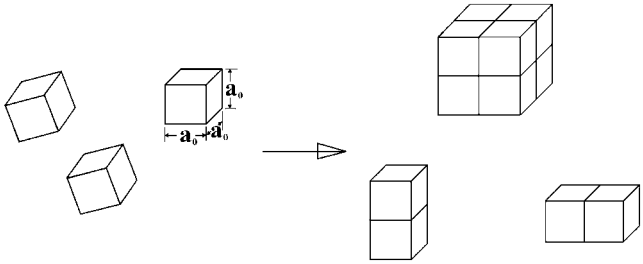


FIG. 1. Three-dimensional aggregation of isotropic kinetic units.

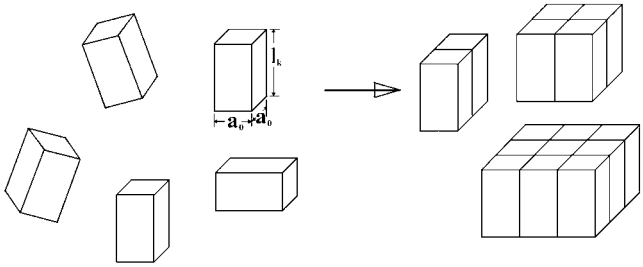


FIG. 2. Two-dimensional aggregation of tetragonal kinetic units.

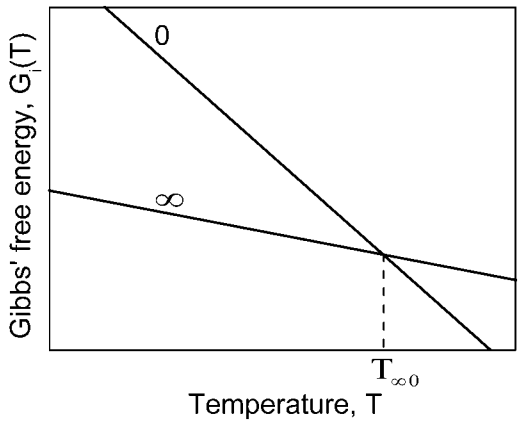


FIG. 3. Gibbs' free energy versus temperature of an ideal two-phase system.

$$G_0(T) = H_0 - T\,S_0,$$
$$G_\infty(T) = H_\infty - T\,S_\infty,$$
$$\Delta G_{\infty 0}(T) = G_0(T) - G_\infty(T) = 0 \Rightarrow T_{\infty 0} = \frac{\Delta H_{\infty 0}}{\Delta S_{\infty 0}} \quad . \tag{1}$$

Thermodynamic potentials of the stable phases (melt 0 and solid ∞) are proportional to volume of the sample, V

$$G_0(T) = V \cdot g_0(T) = V \cdot (h_0 - Ts_0),$$
$$G_\infty(T) = V \cdot g_\infty(T) = V \cdot (h_\infty - Ts_\infty) \quad . \tag{2}$$

The system presented in Fig. 3 provides a reference for the "polymorphic" system containing the melt 0 and several plate-like phases $k = 1, 2, \ldots$ (Fig. 4).

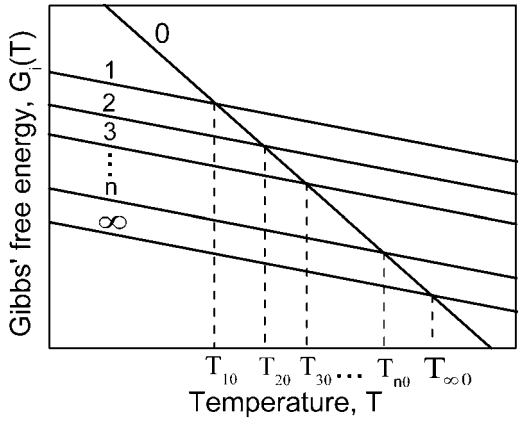


FIG. 4. Gibbs' free energy versus temperature of a multiphase system.

2. A system including several plate-like solid phases

The kinetics of crystallization is described in terms of the many-phase model.[1,13] A system containing solid phases of identical chemical and crystallographic structures, but different enthalpies, is considered. The solid phases consist of plates with different constant thicknesses, l_k. In addition to the plate-like phases, $k = 1, 2, 3, \ldots, n$, the system includes an amorphous (liquid) phase 0 and a reference solid phase ∞ composed of plate-like crystals with infinite thickness. Liquid phase 0 consists of tetragonal kinetic elements of height l_k from which plates of the equivalent thickness l_k are being created.

The plate-like phases exhibit different enthalpies (dependent on the plate thickness l_k) and the same entropies

$$h_k = h_k(l_k) = h_\infty + \delta h_k(l_k),$$
$$s_k = s_\infty = \text{const} \quad k = 1, 2, \ldots \quad , \tag{3}$$

where h_∞ denotes enthalpy density (per unit volume) of the reference solid phase ∞. Free enthalpy of the plate-like phase k consists of two components. One component is proportional to volume V_k and is identical with that of the reference solid ∞. The other one is surface energy proportional to surface area of the plate

$$G_k(T) \cong V_k g_\infty + 2A_k\sigma_e \quad , \tag{4}$$

$$A_k = a_k^2,$$
$$B_k = a_k l_k,$$
$$V_k = a_k^2 l_k \quad . \tag{5}$$

A_k denotes the area of the base face of the plate, $a_k \times a_k$, and σ_e is interface tension on this face. Free enthalpy density of the plate-like phase reads

https://doi.org/10.1557/jmr.2013.74 Published online by Cambridge University Press

$$\frac{G_k(T)}{V_k} = g_\infty(T) + \frac{2\sigma_e}{l_k} = g_k(T),$$
$$g_k(T) \xrightarrow{l_k \to \infty} g_\infty(T) \quad . \tag{6}$$

For the infinitely thick plates, free enthalpy density reduces to that of the reference phase ∞. It is evident that in all temperatures, free enthalpy of the plate-like phases is higher than the reference value and more so the smaller is plate thickness, l_k.

Formation of a plate-like phase k from the liquid phase 0 is controlled by the driving force

$$\Delta g_{0k} = g_k - g_0 = \Delta g_{0\infty} + \frac{2\sigma_e}{l_k} \quad . \tag{7}$$

$\Delta g_{0\infty}$ and Δg_{0k} are negative, and the driving force for crystallization is reduced by positive surface energy. Assuming constant transition entropy crystallization/melting enthalpies and equilibrium transition temperatures are obtained as follows:

$$\begin{aligned}
\Delta g_{0k} &= \Delta g_{0\infty} + \frac{2\sigma_e}{l_k}, \\
\Delta s_{0k} &= \Delta s_{0\infty} < 0, \\
\Delta h_{0k} &= \Delta h_{0\infty} + \frac{2\sigma_e}{l_k} < 0, \\
T_{0\infty} &= T_{\infty 0} = \frac{\Delta h_{0\infty}}{\Delta s_{0\infty}}, \\
T_{0k} &= T_{k0} = \frac{\Delta h_{0k}}{\Delta s_{0k}} = \frac{\Delta h_{0\infty} + \frac{2\sigma_e}{l_k}}{\Delta s_{0\infty}} \\
&= T_{0\infty}\left[1 - \frac{2\sigma_e}{l_k |\Delta h_{0\infty}|}\right] < T_{0\infty} \quad .
\end{aligned} \tag{8}$$

B. Properties and behavior of a plate-like phase

1. Diffusion effects in phase transition processes

An important physical characteristic affecting kinetics of phase transitions is molecular mobility of aggregating/dissociating kinetic units. Transition of phase "i" into phase "j" involves diffusion factor

$$i \to j,$$
$$D_{ij} = \text{const}\ \frac{kT}{h} e^{\frac{-E_D^{ij}}{kT}} \quad . \tag{9}$$

In the case of crystallization, $0 \to k$, diffusion provides transport of kinetic units from the liquid phase to the growing clusters and crystals. Diffusion for direct transitions starting from the ideal liquid phase, D_{0k}, is controlled by molecular motions of the kinetic units, e.g., polymer chain segments, in the liquid phase. Melting of a solid is controlled by motions of small chain fragments splitting from the crystal and disorganizing the crystal structure. For such transitions, diffusion coefficients D_{0k} and D_{k0} are assumed to be finite as in our earlier paper[8]

$$\begin{aligned}
&\text{crystallization } 0 \to k, \\
&D_{0k}(T) = \text{finite}, \\
&\text{melting } k \to 0, \\
&D_{k0}(T) = \text{finite} \quad k = 1, 2, \ldots, n \quad .
\end{aligned} \tag{10}$$

An increase of plate thickness resulting from pulling long polymer chains through viscous medium or doubling plate thickness may require very high transport activation energies. Therefore, in the present model, plate $i \to$ plate j transitions are neglected because of high activation energy

$$\begin{aligned}
&\text{plate } i \leftrightarrow \text{plate } j, \\
&D_{ij} = 0 \quad i,j = 1, 2, \ldots \quad .
\end{aligned} \tag{11}$$

2. Interface tensions

Another material characteristic that should be defined is interface tension, σ. The ranges of σ for isotactic polypropylene are given in Table I. According to Turnbull[14] interface tension, σ_{0k} between the melt, 0, and the kth plate is controlled by structure of the latter. Assuming identical crystallographic structures of various plate-like phases k yields equal solid–melt interface tensions:

$$\begin{aligned}
&\text{solid } k \leftrightarrow \text{melt } 0, \\
&\sigma_{0k} = \sigma_e \quad \text{on the base face, } a_k \times a_k, \\
&\sigma_{0k} = \sigma_s \quad \text{on the side face, } a_k \times l_k \quad k = 1, 2, \ldots \quad ,
\end{aligned} \tag{12}$$

σ_e—surface tension of the base face—is usually much higher than that on the side face, σ_s. Tetragonal symmetry and the surface tensions are also conserved in plate-like clusters.

C. Crystallization and melting rates

1. Formation and melting of a set of plate-like solid phases

Nucleation and growth of plate-like crystals involves reduced number of the degrees of freedom as compared with the reference solid ∞. In contrast to aggregation of isotropic kinetic units (Fig. 1), in the plate-like model, it is assumed that the aggregating units of the amorphous phase (molecules, chain segments, folded-chain units, etc) are considered as tetragonal parallelepipeds with dimensions $l_k \times a_0 \times a_0$ (Fig. 2). After aggregation, primary, three-dimensional clusters with tetragonal symmetry and dimensions $l_k \times a_k \times a_k$ are obtained.

https://doi.org/10.1557/jmr.2013.74 Published online by Cambridge University Press

TABLE I. Material characteristics for α-polypropylene.

Parameter	Characteristic	Value (range)	Source
$T_{\infty 0}$ (K)	Melting temperature	485.2	8,19
$\Delta h_{\infty 0}$ (J/cm^3)	Heat of melting	198.2	8
E_D^{0k} (kJ/mol)	Activation energy in the melt 0	50.2–70.5	8,20
σ_e (J/cm^2)	Interface tension on plate surface	$(6.23 - 12.2) \times 10^{-6}$	8,19
σ_s (J/cm^2)	Interface tension on plate sides	1.15×10^{-6}	21
a_0 (cm)	Side dimension of a kinetic unit	5.817×10^{-8}	Calculated

2. Primary nucleation of plate-like clusters with constant thickness

Free enthalpy of formation primary cluster with finite dimensions $l_k \times a_k \times a_k$ from single kinetic units $l_k \times a_0 \times a_0$ reads

$$\begin{aligned}
&\Delta G_{0k,\mathrm{nuc}} = \left(\Delta g_{0\infty} + \frac{2\sigma_e}{l_k}\right) v_k + 4(v_k l_k)^{1/2}\sigma_s,\\
&\frac{d\Delta G_{0k,\mathrm{nuc}}}{dv_k} = \Delta g_{0\infty} + 2\sigma_e/l_k + 2\sigma_s l_k^{1/2} v_k^{-1/2} = \Delta g_{0k} + 2\sigma_s l_k^{1/2} v_k^{-1/2},\\
&\frac{d\Delta G_{0k,\mathrm{nuc}}}{dv_k} = 0 \Rightarrow \begin{cases} v_k = v_k^* & v_k^* = \frac{4 l_k \sigma_s^2}{(\Delta g_{0\infty} + 2\sigma_e/l_k)^2} = \frac{4\, l_k \sigma_s^2}{\Delta g_{0k}^2},\\ a_k = a_k^* & a_k^* = \frac{-2\sigma_s}{\Delta g_{0k}},\\ \Delta G_{0k,\mathrm{nuc}} = \Delta G_{0k,\mathrm{nuc}}^* & \Delta G_{0k,\mathrm{nuc}}^* = \frac{4 l_k \sigma_s^2}{-(\Delta g_{0\infty} + 2\sigma_e/l_k)} = \frac{-4 l_k \sigma_s^2}{\Delta g_{0k}} \end{cases}.
\end{aligned} \tag{14}$$

Differentiation of the free enthalpy with respect to volume v_k or lateral dimension, a_k, yields critical characteristics of primary plate-like nucleation

The critical free enthalpy, ΔG^*, providing potential barrier for aggregation depends on the plate thickness, l_k. Differentiation of ΔG^* with respect to l_k yields the minimum value of the critical energy, $\Delta G_{\min}^*$, and the optimum value of the parameter l_k

$$\begin{aligned}
&\Delta G_{0k,\mathrm{nuc}}^*(l_k) = \frac{4 l_k \sigma_s^2}{-(\Delta g_{0\infty} + 2\sigma_e/l_k)} = \frac{-4 l_k \sigma_s^2}{\Delta g_{0k}},\\
&\frac{d\Delta G_{0k,\mathrm{nuc}}^*}{dl_k} = \frac{-4\sigma_s^2(\Delta g_{0\infty} + 4\sigma_e/l_k)}{(\Delta g_{0\infty} + 2\sigma_e/l_k)^2} = \frac{-4\sigma_s^2[\Delta g_{0k} + 2\sigma_e/l_k]}{\Delta g_{0k}^2},\\
&\frac{d\Delta G_{0k,\mathrm{nuc}}^*}{dl_k} = 0 \Rightarrow \begin{cases} l_k = l_{\mathrm{opt}} & l_{\mathrm{opt}}(T) = \frac{-4\sigma_e}{\Delta g_{0\infty}(T)},\\ \Delta G_{0k,\mathrm{nuc}}^* = \Delta G_{0k,\mathrm{nuc,opt}}^* & \Delta G_{0k,\mathrm{nuc,opt}}^*(T) = \frac{32\sigma_e\sigma_s^2}{\Delta g_{0\infty}^2(T)} \end{cases}.
\end{aligned} \tag{15}$$

$$\begin{aligned}
&v_k = a_k^2 l_k \quad l_k = \mathrm{const},\\
&\Delta g_{0k} = \Delta g_{0\infty} + \frac{2\sigma_e}{l_k},\\
&\Delta G_{0k,\mathrm{nuc}}(a_k; l_k) = \Delta g_{0\infty} \cdot a_k^2 l_k + 2a_k^2\sigma_e\\
&\qquad + 4\sigma_s a_k l_k = \left(\Delta g_{0\infty} + \frac{2\sigma_e}{l_k}\right) v_k\\
&\qquad + 4\,(v_k l_k)^{1/2}\sigma_s \quad .
\end{aligned} \tag{13}$$

It is interesting to note that the minimum potential barrier to primary nucleation of plates is controlled by geometrically mean interface tension $\bar{\sigma}_{0k} = (\sigma_e \sigma_s^2)^{1/3}$.

In addition to the optimum plate thickness, l_{opt}, which corresponds to the smallest potential barrier $\Delta G_{0k,\mathrm{nuc}}^*$, there appear two other characteristic values of plate thickness l_k. One is the thermodynamic limit, $l_{\min}$, appearing when the free enthalpy of aggregation density, Δg_{0k}, disappears

https://doi.org/10.1557/jmr.2013.74 Published online by Cambridge University Press

$$\Delta g_{0k}(T) = \Delta g_{0\infty}(T) + \frac{2\sigma_e}{l_k} = 0,$$
$$l_k(T) = l_{\min} = \frac{-2\sigma_e}{\Delta g_{0\infty}(T)},$$
$$T(l_{\min}) = T_{0k} \quad , \tag{16}$$

where $T_{0k} = T_{k0}$ is equilibrium melting temperature for phase k. It is obvious that above T_{0k} crystallization of phase k is impossible.

The other (upper) limit of l_k is associated with the conditions when critical volume of the plate $v_k^*(l_k)$ is equal to the volume of two kinetic units, $2v_{0k}$. Using Eq. (14), one obtains

$$v_k^* = \frac{4l_k\sigma_s^2}{\Delta g_{0k}^2} = \frac{4l_k\sigma_s^2}{(\Delta g_{0\infty} + 2\sigma_e/l_k)^2},$$
$$\frac{v_k^*}{v_0} = 2 \Rightarrow l = l_{\max}(T),$$
$$l_{\max}(T) = \frac{-2\sigma_e a_0}{\sqrt{2}\sigma_s + a_0\Delta g_{0\infty}(T)},$$
$$\Delta g_{0\infty}(T) = -\frac{2\sigma_e}{l_{\max}} - \frac{\sqrt{2}\sigma_s}{a_0},$$
$$T(l_{\max}) = T_{0\infty}\left[1 + \left(\frac{2\sigma_e}{l_{\max}} + \frac{\sqrt{2}\sigma_s}{a_0}\right)\frac{1}{\Delta h_{0\infty}}\right] \quad . \tag{17}$$

The conditions described by Eq. (17) determine the upper limit of plate thickness l_k when nucleation-controlled crystallization theory fails. Above $l_k = l_{\max}$, all clusters are capable of infinite growth and nucleation does not play any role in the kinetics.

$$v_k^*(T) \geq 2v_{0k} \quad \text{nucleation-controlled transition},$$
$$v_k^*(T) < 2v_{0k} \quad \text{no nucleation transition} \quad . \tag{18}$$

Primary nucleation rate is controlled by cluster distribution function $\rho_{0k}(v)$ in the vicinity of critical volume, $v_{0k} = v_k^*$. With the "diffusion coefficient" in the form

$$P(a_k^*) = \frac{4a_k^*}{a_{0k}} = \frac{8\sigma_s}{a_{0k}|\Delta g_{0k}|}; \quad a_{0k} = (v_{0k}/l_k)^{1/2},$$
$$D(a_k^*) = P(a_k^*)v_{0k}^2\frac{kT}{h}e^{\frac{-E_D}{kT}}$$
$$= \frac{8\sigma_s l_k^{1/2} v_{0k}^{3/2}}{(|\Delta g_{0\infty}| - 2\sigma_e/l_k)}\frac{kT}{h}e^{\frac{-E_D}{kT}} \quad , \tag{19}$$

steady-state distribution of plate-like clusters derived from the approximation of Frenkel[15] and Zeldovich[16] reads

$$\rho_{st}(v_k) = \frac{1}{2}\rho_{0k}\, e^{\frac{-\Delta G(v_k)}{kT}}\{1 - erf[Z(v_k - v_k^*)]\},$$
$$\rho_{st}(v*) = \frac{1}{2}\rho_{0k}\, e^{\frac{-\Delta G_{0k}}{kT}}$$
$$= \frac{1}{2}\rho_{0k}\exp\left[\frac{-4l_k\sigma_s^2}{kT\cdot[|\Delta g_{0\infty}| - 2\sigma_e/l_k]}\right],$$
$$\left.\frac{\partial\rho_{st}}{\partial v_k}\right|_{v=v*} = \frac{-Z}{\sqrt{\pi}}\rho_{0k}\, e^{\frac{-\Delta G_{0k}}{kT}}$$
$$= \frac{-\rho_{0k}[|\Delta g_{0\infty}| - 2\sigma_e/l_k]^{3/2}}{8\sigma_s\sqrt{\pi kT}l_k^{1/2}}$$
$$\times \exp\left[\frac{-4l_k\sigma_s^2}{kT(|\Delta g_{0\infty}| - 2\sigma_e/l_k)}\right] \quad . \tag{20}$$

Primary nucleation rate of plate-like crystals appears in the form

$$\dot{N}_{0k}(T) = -D(v_k^*)\rho_{0k}\left.\frac{\partial\rho_{st}}{\partial v}\right|_{v*}$$
$$= \frac{(-\Delta g_{0k})^{1/2}\rho_{0k}^2 v_{0k}^{3/2}}{\sqrt{\pi kT}}\frac{kT}{h}\, e^{\frac{-E_D}{kT}}\exp\left[\frac{4l_k\sigma_s^2}{kT\Delta g_{0k}}\right]$$
$$= \frac{(-\Delta g_{0\infty} - 2\sigma_e/l_k)^{1/2}\rho_{0k}^2 v_{0k}^{3/2}}{\sqrt{\pi kT}}\frac{kT}{h}\, e^{\frac{-E_D}{kT}}$$
$$\times \exp\left[\frac{4l_k\sigma_s^2}{kT(\Delta g_{0\infty} + 2\sigma_e/l_k)}\right] \quad . \tag{21}$$

Plate thickness l_k in Eq. (21) cannot be smaller than the minimum value corresponding to zero driving force

$$\Delta g_{0k} = \Delta g_{0\infty} + 2\sigma_e/l_k < 0,$$
$$l_{\min} = -2\sigma_e/\Delta g_{0\infty} \quad . \tag{22}$$

Plates thinner than $l_{\min}$ cannot be created for thermodynamic reasons. It is interesting to note [Eq. (15)] that plate thickness equal to double $l_{\min}$ corresponds to minimum energy barrier of nucleation. Primary nucleation rate is a function of temperature and plate thickness, l_k.

3. Growth of plate-like clusters with constant thickness

Growth of plate-like clusters is reduced to two dimensions parallel to the $a \times a$ surface. Secondary nuclei (nuclei of growth) are attached to side faces $l_k \times a$ of the plate and grow in the dimensions, a. The kinetic unit attached is $l_k \times a_0 \times a_0$. The secondary cluster has a constant thickness, l_k, constant width, a_0, and variable lateral dimension, a. Addition of the first kinetic element ($l_k \times a_0 \times a_0$) to the side face of the crystal plate changes cluster free enthalpy by

https://doi.org/10.1557/jmr.2013.74 Published online by Cambridge University Press

$$
\begin{aligned}
&a = 0 \rightarrow a = a_0,\\
&v_{0k} = a_0^2 l_k,\\
&\Delta G_{0k,\mathrm{gr}}(v_{0k}) = \Delta g_{0\infty} l_k a_0^2 + 2\sigma_e a_0^2 + 2\sigma_s l_k a_0\\
&\qquad = \left(\Delta g_{0\infty} + \frac{2\sigma_e}{l_k}\right) v_{0k} + 2\sigma_s l_k^{1/2} v_{0k}^{1/2} \quad .
\end{aligned} \tag{23}
$$

Free enthalpy of the cluster composed of more than one element and width a reads

$$
\begin{aligned}
&a > a_0,\\
&v = l_k a_0 a; a = \frac{v}{a_0 l_k},\\
&\Delta G_{0k,\mathrm{gr}}(v) = \left(\Delta g_{0\infty} + \frac{2\sigma_e}{l_k}\right) v + 2\sigma_s (l_k v_{0k})^{1/2} \quad .
\end{aligned} \tag{24}
$$

Continualized free enthalpy in the entire range of cluster sizes results in the form of two linear functions of volume, v, increasing in the range of small volumes and decreasing in the range of large v.

$$
\Delta G_{0k,\mathrm{gr}}(v) = \begin{cases}
\left(\Delta g_{0\infty} + \frac{2\sigma_e}{l_k} + 2\sigma_s l_k^{1/2} v_{0k}^{-1/2}\right) v & \text{for } 0 \le v < v_{0k},\\
\Delta G_{0k,\mathrm{gr,max}} = \left(\Delta g_{0\infty} + \frac{2\sigma_e}{l_k}\right) v_{0k} + 2\sigma_s l_k^{1/2} v_{0k}^{1/2} & \text{for } v = v_{0k},\\
\left(\Delta g_{0\infty} + \frac{2\sigma_e}{l_k}\right) v + 2\sigma_s l_k^{1/2} v_{0k}^{1/2} & \text{for } v > v_{0k}.
\end{cases} \tag{25}
$$

Of course, the range $v < v_{0k}$ (cluster size smaller than that of a single kinetic unit) does not have physical sense.

Maximum free enthalpy of secondary clusters, providing thermodynamic barrier for crystal growth corresponds to deposition of a single kinetic unit: $v^* = v_{0k}$. Formal differentiation of free enthalpy with respect to cluster volume yields different values for small and large clusters. The gradient $\mathrm{d}\Delta G_{0k,\mathrm{gr}}/\mathrm{d}v$ is indefinite at $v = v_{0k}$

$$
\frac{\mathrm{d}\Delta G_{0k,\mathrm{gr}}}{\mathrm{d}v} = \begin{cases}
-|\Delta g_{0\infty}| + \frac{2\sigma_e}{l_k} + \sigma_s l_k^{1/2} v_{0k}^{-1/2} \ge 0 & \text{for } v < v_{0k},\\
\text{Indefinite} & \text{for } v = v_{0k},\\
-|\Delta g_{0\infty}| + \frac{2\sigma_e}{l_k} \le 0 & \text{for } v > v_{0k} \quad .
\end{cases} \tag{26}
$$

In contrast to primary nucleation, form of the free enthalpy gradient [Eq. (26)], excludes the possibility of describing plate-crystal growth in terms of the continuous cluster distribution function, $\rho(v)$.

The problem of crystal growth has been solved by Hoffman and Lauritzen,[10–12] Frank and Tosi,[17] and other authors on the basis of a discrete system of bimolecular association–dissociation reactions. Free enthalpy of a q-element cluster formed from $a \times b \times l_k$ parallelepiped units

$$
\begin{aligned}
\Delta F(q) &= 2bl\sigma_s + 2qab\sigma_e - qabl\Delta f,\\
v_{0k} &= abl
\end{aligned} \tag{27}
$$

translated to our symbols

$$
\begin{aligned}
\Delta F &= \Delta G(v),\\
q &= v/v_{0k},\\
b &= a_0,\\
a &= a_0,\\
\Delta f &= -\Delta g_{0\infty},\\
v_{0k} &= a_0^2 l_k,\\
a_0 &= \left(\frac{v_{0k}}{l_k}\right)^{1/2}
\end{aligned} \tag{28}
$$

yields free enthalpy

$$
\Delta G_{0k,\mathrm{gr}}(v) = \left(\Delta g_{0\infty} + \frac{2\sigma_e}{l_k}\right) v + 2\sigma_s (v_{0k} l_k)^{1/2} \tag{29}
$$

identical to that derived in this paper for large volumes [Eq. (25)]. Solving a discrete system of association–dissociation reactions Hoffman et al.[12] obtained the flux of secondary nuclei at $v = v_{0k}$ in the form

$$
\begin{aligned}
S(l)/N_0 &= \beta \exp\left[\frac{-2bl\sigma_s + \psi abl\Delta f}{kT}\right]\\
&\quad \times \left\{1 - \exp\left[\frac{-abl\Delta f + 2ab\sigma_e}{kT}\right]\right\},\\
\beta &= \frac{kT}{h} J_1 \exp\left[\frac{-U*}{R(T - T_\infty)}\right];\\
T_\infty &= T_g - 30, \quad \psi \in \langle 0, 1\rangle \quad ,
\end{aligned} \tag{30}
$$

where ψ is a model parameter.[12] For the discussion of plate-like crystallization, it will be assumed

$$
J_1 = 1; \quad \psi = 1; \quad \beta = \frac{kT}{h} \mathrm{e}^{\frac{-E_D}{kT}} \quad . \tag{31}
$$

The Williams-Landel-Ferry (WLF) formula in Eq. (30) will be replaced with an Arrhenius mobility barrier.

https://doi.org/10.1557/jmr.2013.74 Published online by Cambridge University Press

Assumption $\psi = 1$ corresponds to direct attachment of kinetic elements of the amorphous phase to the cluster. With these conditions, substituted to Eq. (30), the flux is obtained in the form as follows:

$$S(l)/N_0 = \frac{kT}{h}\,\mathrm{e}^{\frac{-E_D}{kT}} \exp\left[\frac{-2(v_{0k}l_k)^{1/2}\sigma_s + v_{0k}|\Delta g_{0\infty}|}{kT}\right] \times \left\{1 - \exp\left[\frac{-v_{0k}|\Delta g_{0k}|}{kT}\right]\right\},$$
$$|\Delta g_{0k}| = |\Delta g_{0\infty}| - \frac{2\sigma_e}{l_k} < |\Delta g_{0\infty}| \quad . \tag{32}$$

Linear growth rate, $\dot{R}_{0k}$, in the direction normal to the edge face ($l_k \times a$) results as

$$\dot{R}_{0k} = a_0 \cdot S(l_k)/N_0 = (v_{0k}/l_k)^{1/2}\frac{kT}{h}\,\mathrm{e}^{\frac{-E_D}{kT}} \times \exp\left[\frac{-2(v_{0k}l_k)^{1/2}\sigma_s + v_{0k}|\Delta g_{0\infty}|}{kT}\right] \times \left\{1 - \exp\left[\frac{-v_{0k}|\Delta g_{0k}|}{kT}\right]\right\} \quad . \tag{33}$$

D. Global transition rates

1. Formation of a simple plate-like phase

Let us start with a simple plate-like crystal phase in which all plates have the same thickness, l_k. Taking into account, primary nucleation rate from Eq. (21) and growth rate from Eq. (33), the progress function $E(t)$ for sporadic nucleation results as follows:

$$E_{0k}^{\mathrm{spc}}(t) = l_k \cdot \int_0^t \dot{N}_{0k}(s)\left[\int_s^t \dot{R}_{0k}(z)\mathrm{d}z\right]^2 \mathrm{d}s \xrightarrow{\text{isothermal}} \frac{1}{3} \times \dot{N}_{0k} \cdot l_k \cdot \dot{R}_{0k}^2 t^3 = \frac{|\Delta g_{0k}|^{1/2} v_{0k}^{1/2}}{3\sqrt{\pi kT}}\left(\frac{kT}{h}\,\mathrm{e}^{\frac{-E_D}{kT}}\right)^3 \exp\left[\frac{-4l_k\sigma_s^2}{kT|\Delta g_{0k}|}\right] \times \exp\left[\frac{-4(v_{0k}l_k)^{1/2}\sigma_s + 2v_{0k}|\Delta g_{0\infty}|}{kT}\right] \times \left\{1 - \exp\left[\frac{-v_{0k}|\Delta g_{0k}|}{kT}\right]\right\}^2 t^3 \quad , \tag{34}$$

and the frequency function $\nu(t)$

$$\nu_{0k}^{\mathrm{spc}} = (E_{0k}^{\mathrm{spc}}/t^3)^{1/3} = \frac{|\Delta g_{0k}|^{1/6}\nu_{0k}^{1/6}}{3^{1/3}(\pi kT)^{1/6}}\left(\frac{kT}{h}\,\mathrm{e}^{\frac{-E_D}{kT}}\right)\exp\left[\frac{-4l_k\sigma_s^2}{3kT|\Delta g_{0k}|}\right] \times \exp\left[\frac{-4(\nu_{0k}l_k)^{1/2}\sigma_s + 2\nu_{0k}|\Delta g_{0\infty}|}{3kT}\right] \times \left\{1 - \exp\left[\frac{-\nu_{0k}|\Delta g_{0k}|}{kT}\right]\right\}^{2/3} \quad . \tag{35}$$

E. Development of phase composition

1. Direct amorphous–solid transitions

Isothermal crystallization of an undercooled amorphous phase 0 into a single solid phase k ($k = 1, 2, 3$) at $T < T_{k0}$ yields time-dependent composition vector, x

$$\begin{pmatrix} x_0(t=0) = x_0^0 \\ x_k(t=0) = x_k^0 \end{pmatrix} = \begin{pmatrix} 1 \\ 0 \end{pmatrix} \xrightarrow{E_{0k}(t)} \begin{pmatrix} \mathrm{e}^{-E_{0k}(t)} \\ 1 - \mathrm{e}^{-E_{0k}(t)} \end{pmatrix} \xrightarrow{t\to\infty} \begin{pmatrix} 0 \\ 1 \end{pmatrix} \tag{36}$$

and isothermal melting of the solid phase k at $T > T_{k0}$

$$\begin{pmatrix} x_k^0 = 1 \\ x_0^0 = 0 \end{pmatrix} = \begin{pmatrix} 1 \\ 0 \end{pmatrix} \xrightarrow{E_{k0}(t)} \begin{pmatrix} \mathrm{e}^{-E_{k0}(t)} \\ 1 - \mathrm{e}^{-E_{k0}(t)} \end{pmatrix} \xrightarrow{t\to\infty} \begin{pmatrix} 0 \\ 1 \end{pmatrix} \quad . \tag{37}$$

2. Simultaneous isothermal crystallization of three plate-like solids from the amorphous phase

It is evident that primary nucleation rates $\dot{N}_{0k}$, linear growth rates $\dot{R}_{0k}$, and global progress functions E_{0k}^{spc} depend on plate thickness, l_k. For isolated direct transitions, $0 \to k$, starting from an undiluted amorphous phase, all single kinetic units are assumed to have the same length l_k. Consequently, the concentration ρ_{0k} of effective kinetic units is equal to reciprocal volume of the unit

$$\text{isolated transition } 0 \to k, \qquad \rho_{0k} = \frac{1}{v_{0k}} \quad \text{for } k = 1, 2, \ldots, n \quad . \tag{38}$$

When different plate-like transitions take place simultaneously, a mixture of plate-like crystals is obtained. It is

https://doi.org/10.1557/jmr.2013.74 Published online by Cambridge University Press

assumed that direct plate-plate transitions $i \rightarrow j$ are excluded for kinetic reasons [see Eq. (11)]. The basic postulate of the model—constant plate thickness for each species—requires existence of different kinetic elements in the source (amorphous) phase. Such a situation may be viewed as a mixture of different amorphous phases, {"0_k"} crystallizing into separate plate-like solids, l_k. Kinetic elements with length l_k (volume v_{0k}) occupy a fraction f_k of the total volume of the amorphous phase

$$\begin{aligned} &\text{simultaneous transitions } 0_k \rightarrow k, \\ &\rho_{0k} v_{0k} = f_k, \\ &\rho_{01} v_{01} + \rho_{02} v_{02} + \cdots + \rho_{0n} v_{0n} = \sum_{k=1}^{n} f_k = 1, \\ &\rho_{0k} = \frac{f_k}{v_{0k}} \quad , \end{aligned} \tag{39}$$

where ρ_{0k} is the initial concentration of single elements effective in the creation of phase k, and f_k is a fraction of the k-type kinetic units in the amorphous phase.

The progress function of the transition $0 \rightarrow k$ reads

$$\begin{aligned} E_{0k}^{\mathrm{spc}}(t) = &\frac{|\Delta g_{0k}|^{1/2} \rho_{0k}^2 v_{0k}^{5/2}}{3\sqrt{\pi k T}} \left(\frac{kT}{h}\, \mathrm{e}^{\frac{-E_D}{kT}} \right)^3 \\ &\times \exp\left[\frac{-4 l_k \sigma_s^2}{kT|\Delta g_{0k}|} \right] \\ &\times \exp\left[\frac{-4 (v_{0k} l_k)^{1/2} \sigma_s + 2 v_{0k} |\Delta g_{0\infty}|}{kT} \right] \\ &\times \left\{ 1 - \exp\left[\frac{-v_{0k} |\Delta g_{0k}|}{kT} \right] \right\}^2 t^3 \quad . \end{aligned} \tag{40}$$

Simultaneous creation of n plate-like phases from the amorphous phase requires considering n appropriate amorphous phases $0_1, 0_2, \ldots, 0_n$. The progress function for an isolated transition $0_k \rightarrow k$ is obtained in the form

$$\begin{aligned} E_{0k}^{\mathrm{spc}}(t) = &\frac{|\Delta g_{0k}|^{1/2} v_{0k}^{1/2} f_k^2}{3\sqrt{\pi k T}} \left(\frac{kT}{h} \mathrm{e}^{\frac{-E_D}{kT}} \right)^3 \exp\left[\frac{-4 l_k \sigma_s^2}{kT|\Delta g_{0k}|} \right] \\ &\times \exp\left[\frac{-4 (v_{0k} l_k)^{1/2} \sigma_s + 2 v_{0k} |\Delta g_{0\infty}|}{kT} \right] \\ &\times \left\{ 1 - \exp\left[\frac{-v_{0k} |\Delta g_{0k}|}{kT} \right] \right\}^2 t^3 \quad . \end{aligned} \tag{41}$$

where f_k is a material characteristic. Square of f_k appears in Eq. (41) because nucleation and crystal growth processes are controlled by bimolecular reactions of kinetic elements. Assuming, for simplicity, equal volume fractions of single elements

$$f_k = v_{0k} \rho_{0k} = \frac{1}{n} \quad , \tag{42}$$

one obtains

$$\begin{aligned} E_{0k}^{\mathrm{spc}}(t) = &\frac{|\Delta g_{0k}|^{1/2} v_{0k}^{1/2}}{3 n^2 \sqrt{\pi k T}} \left(\frac{kT}{h}\, \mathrm{e}^{\frac{-E_D}{kT}} \right)^3 \exp\left[\frac{-4 l_k \sigma_s^2}{kT|\Delta g_{0k}|} \right] \\ &\times \exp\left[\frac{-4 (v_{0k} l_k)^{1/2} \sigma_s + 2 v_{0k} |\Delta g_{0\infty}|}{kT} \right] \\ &\times \left\{ 1 - \exp\left[\frac{-v_{0k} |\Delta g_{0k}|}{kT} \right] \right\}^2 t^3 \quad . \end{aligned} \tag{43}$$

What is the physical basis for the existence of kinetic units with different lengths l_k? In the case of long-chain polymers, one can identify kinetic units with locally ordered chain fragments (chain folds, extended chain segments, etc.). The characteristic length of rigid rod-like oligomers can be controlled by their molecular mass.

Combination of three simultaneous transitions (three amorphous phases into three solid phases) yields

$$\begin{aligned} &\begin{pmatrix} x_{01}^0 = f_1 \\ x_{02}^0 = f_2 \\ x_{03}^0 = f_3 \\ x_1^0 = 0 \\ x_2^0 = 0 \\ x_3^0 = 0 \end{pmatrix} \rightarrow \begin{pmatrix} x_{01}(t) \\ x_{02}(t) \\ x_{03}(t) \\ x_1(t) \\ x_2(t) \\ x_3(t) \end{pmatrix} = \begin{pmatrix} f_1\, \mathrm{e}^{-E_{01,1}} \\ f_2\, \mathrm{e}^{-E_{02,2}} \\ f_3\, \mathrm{e}^{-E_{03,3}} \\ f_1(1 - \mathrm{e}^{-E_{01,1}}) \\ f_2(1 - e^{-E_{02,2}}) \\ f_3(1 - e^{-E_{03,3}}) \end{pmatrix}; \\ &f_1 + f_2 + f_3 = 1 \quad . \end{aligned} \tag{44}$$

Asymptotically

$$\begin{pmatrix} x_{01}(t) \\ x_{02}(t) \\ x_{03}(t) \\ x_1(t) \\ x_2(t) \\ x_3(t) \end{pmatrix} \xrightarrow{t=\infty, E_{0k,k}=\infty} \begin{pmatrix} 0 \\ 0 \\ 0 \\ f_1 \\ f_2 \\ f_3 \end{pmatrix} \quad , \tag{45}$$

where $E_{0k,k}$ denotes progress function of the transition $0_k \rightarrow k$. Phase k saturates at the level f_k equal to fraction of the corresponding amorphous species 0_k. This corresponds to the concept of crystallization with limited amount of crystallizable amorphous phase.[18]

III. EXAMPLE CALCULATIONS

Effects of plate thickness on the kinetics of nucleation, global transition rates, and the resulting phase composition are discussed. The example material considered is

https://doi.org/10.1557/jmr.2013.74 Published online by Cambridge University Press

the isotactic polypropylene discussed in Refs. 1, 8, and 18. Material characteristics collected in Table I correspond to the reference solid ($k = \infty$, infinite plate thickness). Properties of solids with finite plate thicknesses are calculated.

It should be noted that material characteristics appearing in the model are not unique. This is illustrated in Table I showing ranges of activation energies, E_D, and interface tensions σ_e measured by various authors. The differences may be caused by molecular structure of the polymer (average molecular mass, polydispersity), impurities, thermal and mechanical history of the sample, measuring techniques, etc. Therefore, our analysis is aimed at qualitative or semiquantitative features of plate-like crystallization rather than providing exact quantitative material data.

Numerical simulation results presented in Figs. 5–21 involve activation energy $E_D = 70$ kJ/mol and interface tension, $\sigma_e = 1.22 \cdot 10^{-5}$ J/cm^2.

Figure 5 presents melting temperatures of plate-like solids, T_{k0}, as functions of plate thickness, l_k. In the range of plates thinner than 10^{-6} cm doubling of l_k causes increase of melting temperatures by several decades. Melting temperature of thick plates ($l_k > 10^{-5}$ cm) is nearly insensitive to plate thickness. Asymptotically, equilibrium transition temperature $T_{\infty 0}$ for infinitely thick plates is obtained.

Figure 6 presents critical free enthalpy, $\Delta G^*_{0k}/kT$, for primary plate-like nucleation as a function of plate thickness, l_k. At a constant temperature, an increase of plate thickness from l_{min} (corresponding to melting temperature, T_{k0}) makes the potential barrier go down from infinity to a minimum at the optimum thickness, $l_{opt} = 2l_{min}$ [Eq. (15)]. Further increase of thickness causes increase of the barrier. Both thickness characteristics, l_{opt} and l_{min}, increase with increasing temperature (Fig. 7).

$\Delta G^*_{0k,nuc,opt}$ provides optimum conditions for primary nucleation. Temperature dependence of this characteristic is shown in Fig. 8. The optimum free enthalpy increases with increasing temperature and approaches infinity at equilibrium melting temperature, $T_{\infty 0}$.

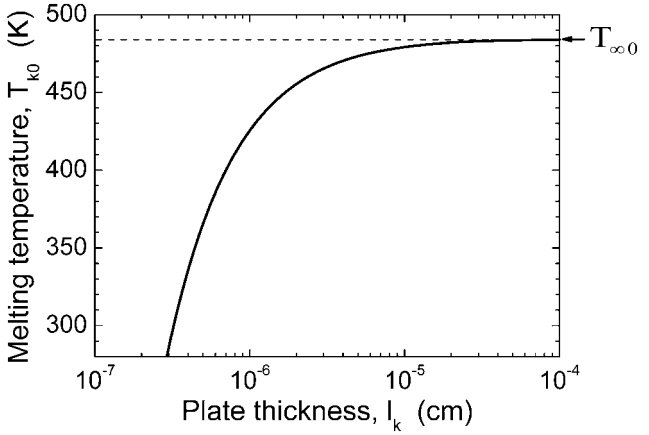


FIG. 5. Melting temperature of plate-like crystals with constant thickness.

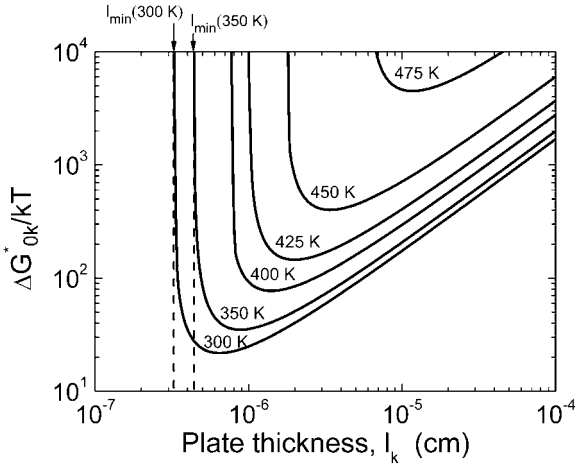


FIG. 6. Critical free enthalpy, $\Delta G^*_{0k}/kT$, as a function of plate thickness, l_k, for plate-like nucleation. Crystallization temperatures indicated.

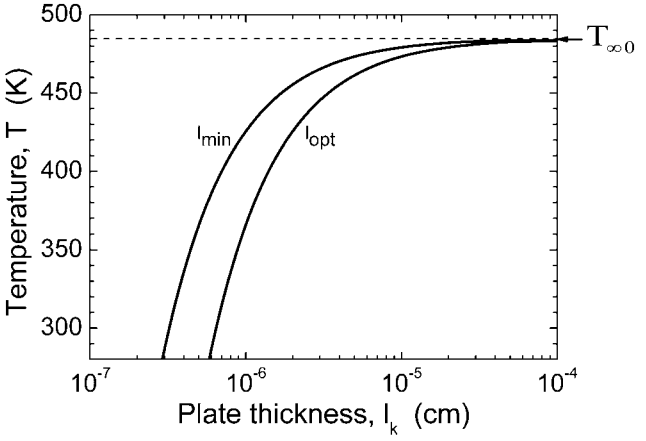


FIG. 7. Temperature dependence of the thickness characteristics l_{min} and l_{opt} for primary plate-like nucleation.

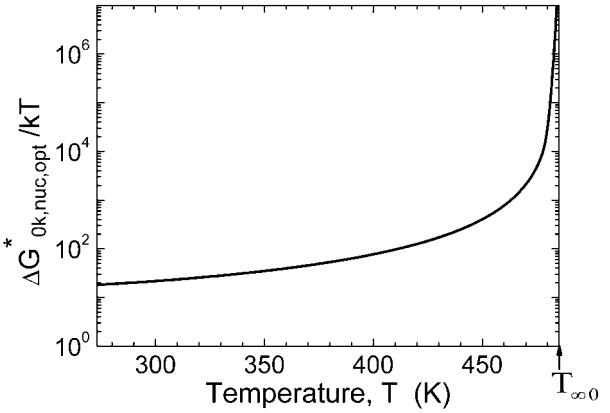


FIG. 8. Minimum value of the critical free enthalpy $\Delta G^*_{0k,nuc,opt}/kT$ as a function of temperature.

https://doi.org/10.1557/jmr.2013.74 Published online by Cambridge University Press

Figure 9 presents a map of nucleation behavior in the "plate-thickness–temperature" space. Minimum plate thickness, $l_{\min}(T)$, corresponds to the situation when the total free enthalpy (including surface and bulk energies) is equal to zero [Eq. (16)]. This condition determines melting temperature of the kth species, T_{k0}. The minimum thickness increases with increasing temperature and approaches infinity at $T = T_{\infty 0}$.

The upper value of plate thickness, $l_{\max}$ [Eq. (17)], corresponds to bounds of the nucleation theory. In the range of thick plates, $l(T) > l_{\max}(T)$, all molecular (atomic) clusters behave like nuclei and can grow to macroscopic dimensions. For the maximum plate thickness, $l_{\max}$, the critical cluster volume is equal to two single units [Eq. (17)]. The situations typical for nucleation-free crystallization include very deep undercooling and crystallization in external potential fields.

Nucleation-controlled crystallization is confined to the plate thickness range $l_{\min}(T) < l_k(T) \leq l_{\max}(T)$. The maximum thickness increases with temperature and approaches infinity at $T_{\max} = T_{0\infty}\left[1 + \left(\frac{\sqrt{2}\sigma_s}{a_0 \Delta h_{0\infty}}\right)\right]$.

The following analysis of the kinetics of plate-like crystallization will be limited to the range of nucleation-controlled transitions. Therefore, in Fig. 10, critical free enthalpy, $\Delta G^*_{0k}/kT$ providing potential barrier for nucleation is truncated on the side of high l_k as related to nucleation-free mechanism.

The frequency ν^{spc}_{0k} involving primary sporadic nucleation and growth [Eq. (35)] is a measure of global transition rate. Isothermal frequency of crystallization from the amorphous phase into plate-like solids is presented in Fig. 11. In the range of low temperatures (280–330 K) the frequency monotonically increases with plate thickness reaching highest values at $l = l_{\max}$. In higher temperatures (Fig. 12), isothermal crystallization frequencies pass through maxima and then decrease with increasing plate thickness l_k.

Figure 13 presents two special values of crystallization frequency, ν^{spc}_{0k}. $\nu[l_{\max}(T)]$ presents the frequency

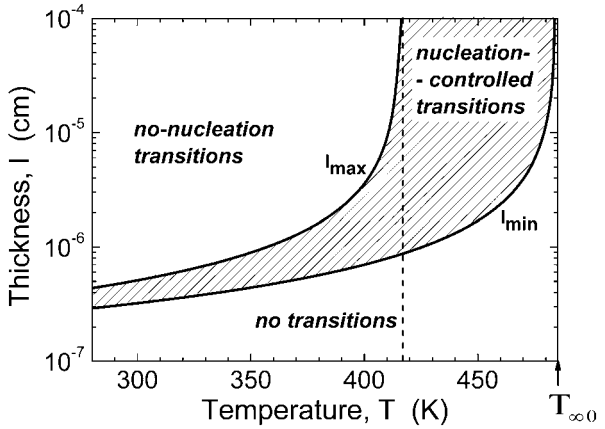


FIG. 9. Characteristic thickness values as functions of temperature.

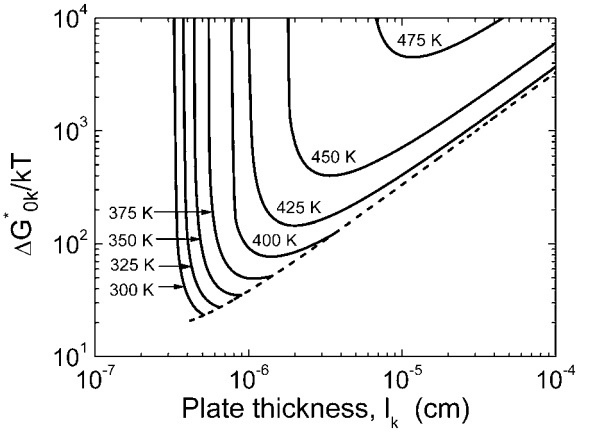


FIG. 10. Critical free enthalpy, $\Delta G^*_{0k}/kT$, as a function of plate thickness, l_k for primary plate-like nucleation. Dash line indicates $l_{\max}$ limit. Crystallization temperatures indicated.

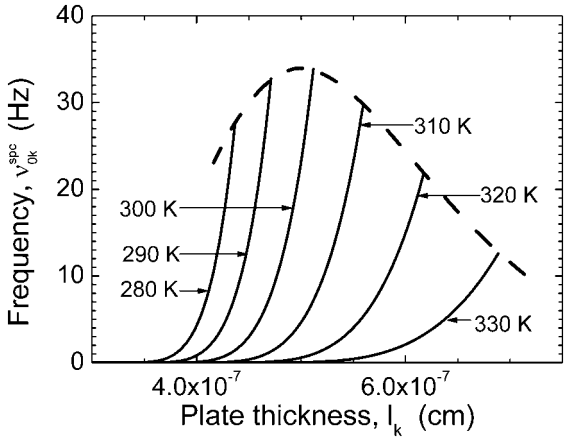


FIG. 11. Isothermal frequency of isolated amorphous–solid transitions. Crystallization temperatures indicated. The limit $l_k = l_{\max}(T)$ at the truncation is represented by dashed line.

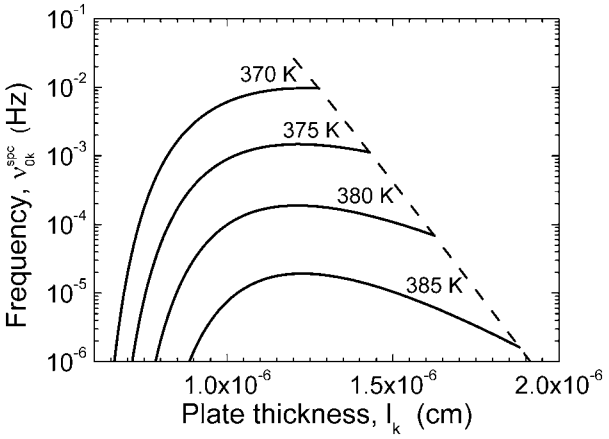


FIG. 12. Isothermal frequency of isolated amorphous–solid transitions. Crystallization temperatures indicated. The limit $l_k = l_{\max}(T)$ at the truncation is represented by dashed line.

https://doi.org/10.1557/jmr.2013.74 Published online by Cambridge University Press

corresponding to maximum plate thickness on the boundary of the nucleation theory. $\nu_{max}(T)$ is obtained directly by differentiating the function $\nu_{0k}^{spc}(T, l_k)$with respect to plate thickness, l_k. Vertical line separates the low temperature region where maximum frequency is achieved for $l_k = l_{max}(T)$ from the high temperature region with maximum frequency $\nu_{max}(T)$. For example, for material characteristics from Table I, maximum crystallization frequency is 34 per s at $T = 297$ K and $l_k = 5.0 \times 10^{-7}$ cm. With increasing temperature, the maximum frequency decreases. Above $T = 390$ K, $\nu_{max}(T)$ drops down below 10^{-6} per s and hardly contributes to sporadically nucleated crystallization kinetics.

Figure 14 shows thickness of plate-like crystals with highest frequency of creation $l(\nu_{max})$. Two temperature regions are separated by a vertical line. In the low temperature region (see Fig. 11, $T_{\infty 0} - T > 140$ K), maximum frequency corresponds to $l_k = l_{max}(T)$. Thick plate-like crystals are created faster than thinner ones. In the high temperature region ($T_{\infty 0} - T < 140$ K), the characteristic $l(\nu_{max})$ moves toward the thermodynamic limit, $l_{min}(T)$. In this region, crystallization frequency passes through a maximum, $l(\nu_{max})$.

Isothermal transition rates for plates of different thicknesses, l_k, are compared in Fig. 15. Creation of plates of a given thickness, l_k, starts at a temperature $T(l_{max})$, where plate thickness corresponds to the boundary of the nucleation mechanism [see Eq. (17)]. With increasing temperature, crystallization frequency $\nu_{0k}^{spc}(T)$ drops down to very small values and disappears at the melting temperature, T_{k0}.

Comparison of the development of phase composition, $x_k(t)$, has been based on the sporadic nucleation mechanism [Eqs. (36) and (44)]. Figures 16, 18, and 20 present

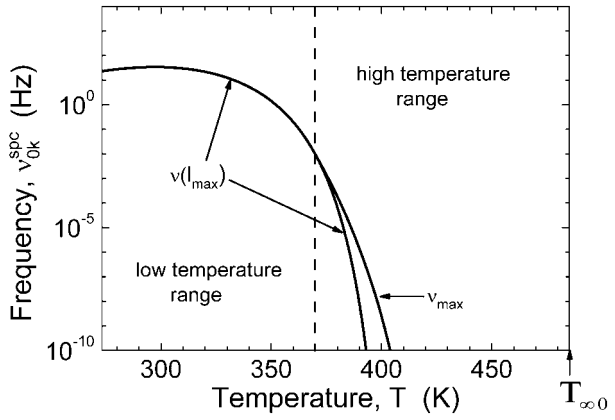


FIG. 13. Maximum values of the isothermal transition frequency versus temperature. Vertical line divides low and high temperature regions (see Figs. 11 and 12).

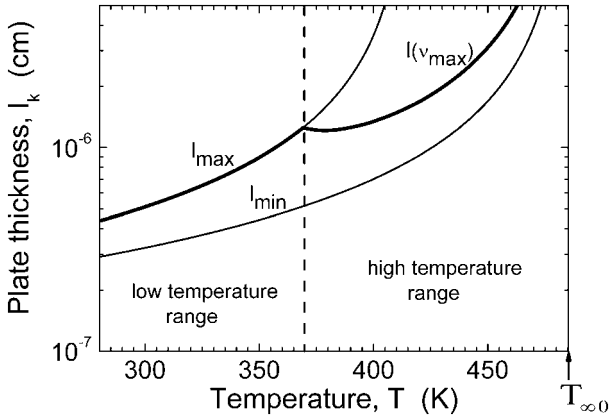


FIG. 14. A map of nucleation behavior for plate-like crystallization. $l_{min}(T)$—minimum plate thickness corresponding to melting temperature T_{k0} [Eq. (16)], $l_{max}(T)$—maximum plate thickness at the transition from nucleation-controlled to no nucleation transition regime, and $l(\nu_{max})$—plate thickness corresponding to maximum crystallization rate. A vertical line divides low and high temperature regions.

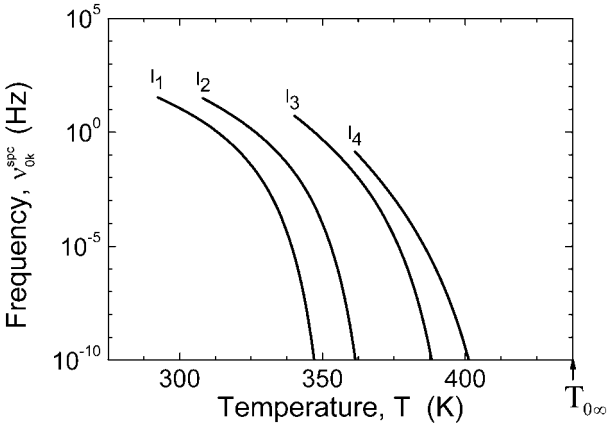


FIG. 15. Frequency of isolated isothermal transitions $0 \rightarrow k$ versus temperature. Plate thickness: $l_1 = 4.8 \times 10^{-7}$ cm, $l_2 = 5.5 \times 10^{-7}$ cm, $l_3 = 7.8 \times 10^{-7}$ cm, and $l_4 = 10.8 \times 10^{-7}$ cm.

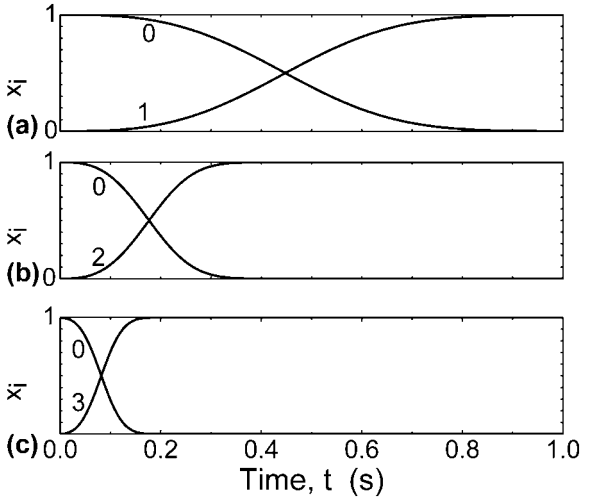


FIG. 16. Isothermal development of phase composition at $T = 305$ K in isolated two-phase systems. 0—amorphous phase, (a) Transition $0 \rightarrow 1$ ($l_1 = 4.6 \times 10^{-7}$ cm), (b) Transition $0 \rightarrow 2$ ($l_2 = 4.8 \times 10^{-7}$ cm), (c) Transition $0 \rightarrow 3$ ($l_3 = 5.0 \times 10^{-7}$ cm).

https://doi.org/10.1557/jmr.2013.74 Published online by Cambridge University Press

the phase content development resulting from isolated transitions $0 \rightarrow k$. Figures 17, 19, and 21 concern simultaneous transitions in a system composed of the "mixed" amorphous phase and three different plate-like solids. Plate thicknesses have been chosen in the region close to maximum transition frequency.

Figures 16 and 17 present development of the amorphous solid composition in the region of low temperatures ($T = 305$ K), where maximum crystallization frequency corresponds to l_{max}. Consequently, creation of thicker plates is faster than that of thinner ones. Saturation of composition for the three selected plates is observed in the period shorter than 1 s.

According to the model, simultaneous creation of several different plate-like phases requires considering amorphous phase 0 as consisting of a corresponding number of different amorphous components "0_1", "0_2", and "0_3." A kth component contains tetragonal parallelepipeds of height l_k and in the process of $0_k \rightarrow$ k transition is converted into plate-like crystals of thickness l_k.

For the sake of simplicity, equal fractions of the amorphous components are assumed, $f_1 = f_2 = \cdots = f_n$. Consequently, in Figs. 17, 19, and 21 asymptotic fractions of the three plate-like solids approach the level $x_k = f_k = 1/3$ and the amorphous phases are fully converted.

In the low temperature region, thicker crystal plates are created faster than thinner ones. Comparing Figs. 16 and 17, one finds that simultaneous creation of several plate-like phases is slower because of dilution of the source (amorphous) phase ($f_k < 1$).

Figures 18–21 present development of phase composition in the high temperature region ($T = 375$ K) where there is no correspondence between maximum plate thickness, l_{max}, and maximum transition frequency, ν_{max}.

Three plates thinner than those created with maximum frequency were selected: At $T = 375$ K, $l(\nu_{max})$ is about 1.22×10^{-6} cm, The thicknesses selected for the kinetic computations are 1.0×10^{-6}, 1.1×10^{-6}, and 1.2×10^{-6} cm. Development of phase composition in isolated transitions $0_k \rightarrow k$ is shown in Fig. 18 and that in a process of three simultaneous transitions in Fig. 19. It is evident that thicker plates crystallize faster than thinner ones.

Development of phase composition in the same temperature (375 K) in a set of plates thicker than $l(\nu_{max})$ are presented in Figs. 20 and 21. The order of creation rates is reversed: thin plates are created faster than thick ones.

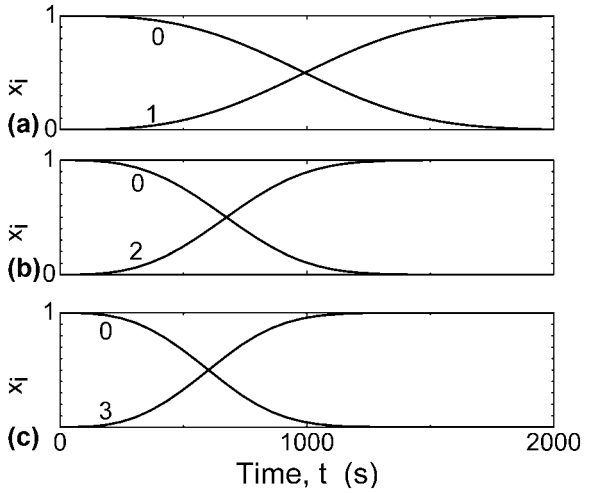


FIG. 18. Isothermal development of phase composition at $T = 375$ K in isolated two phase systems in case of $l_k < l(\nu_{max})$. 0—amorphous phase, (a) Transition $0 \rightarrow 1$ ($l_1 = 1.0 \times 10^{-6}$ cm), (b) Transition $0 \rightarrow 2$ ($l_2 = 1.1 \times 10^{-6}$ cm), (c) Transition $0 \rightarrow 3$ ($l_3 = 1.2 \times 10^{-6}$ cm).

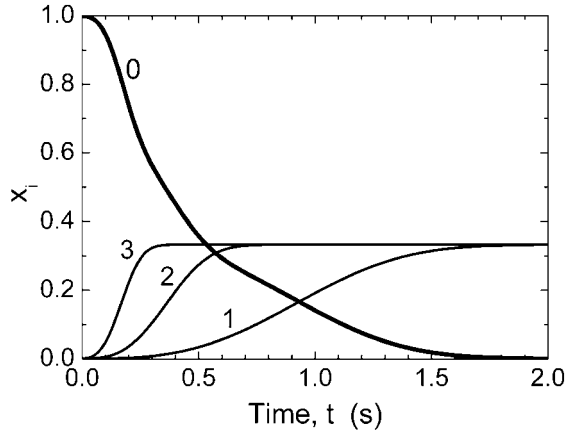


FIG. 17. Simultaneous isothermal development of phase composition at $T = 305$ K for a system containing three plate-like solids. 0—sum of unconverted amorphous phases, 1, 2, 3—plate-like solids. Plate thickness: $l_1 = 4.6 \times 10^{-7}$ cm, $l_2 = 4.8 \times 10^{-7}$ cm, $l_3 = 5.0 \times 10^{-7}$ cm, amorphous fractions assumed $f_1 = f_2 = f_3 = 1/3$.

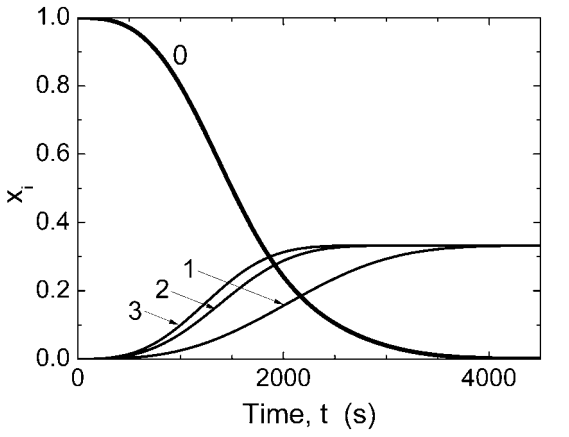


FIG. 19. Simultaneous isothermal development of phase composition at $T = 375$ K for a system containing three plate-like solids in case of $l_k < l(\nu_{max})$. 0—sum of unconverted amorphous phases, 1, 2, 3—plate-like solids. Plate thickness: $l_1 = 1.0 \times 10^{-6}$ cm, $l_2 = 1.1 \times 10^{-6}$ cm, $l_3 = 1.2 \times 10^{-6}$ cm, amorphous fractions assumed $f_1 = f_2 = f_3 = 1/3$.

https://doi.org/10.1557/jmr.2013.74 Published online by Cambridge University Press

Crystallization at $T = 375$ K is much slower than that at 305 K.

IV. DISCUSSION

The main aim of this study was description of the crystallization kinetics based on two-dimensional homogeneous nucleation of crystal plates and their planar growth (constant plate thickness). The amorphous phase was assumed to consist of kinetic units with constant width a_0 and different heights l_k, giving rise to plate-like crystals of predetermined thickness. Enthalpy of a plate-like crystal phase characterized by finite thickness l_k is higher than that of an ideal three-dimensional solid phase ($l_k = \infty$) treated as a reference. Entropy of plate-like solids is assumed a constant, equal to that of the reference phase.

It was shown that thickness of plate-like crystals created in nucleation-controlled processes is limited. The lower thermodynamic limit $l_{\min}(T) = -2\sigma_e/\Delta g_{0\infty}$ is determined by Gibbs' free energy of the transition. The upper limit $l_{\max}(T) = \frac{-2\sigma_e a_0}{\sqrt{2}\sigma_s + a_0 \Delta g_{0\infty}(T)}$ corresponds to the conditions when the critical cluster volume found from the theory of nucleation is equal to two elementary units. Above that limit, all molecular clusters present in the system behave like effective nuclei and are able to grow to macroscopic dimensions. This eliminates sporadic nucleation but does not exclude crystallization involving other mechanisms not covered by the present model.

In each temperature, there is a plate thickness corresponding to highest frequency of the transition. In lower temperature range, maximum crystallization frequency is determined by the nucleation criterion [Eq. (17)]. In Figs. 11 and 12, crystallization frequency, ν_{0k}^{spc}, is plotted versus plate thickness at various temperatures. In the higher temperature range, the frequency functions $\nu_{0k}^{spc}(l_k, T)$pass through maxima (Fig. 12). The frequency functions are truncated by the condition $l = l_{\max}$ and their terminal points are connected with a dashed line. Figure 13 presents crystallization frequency in the wide range of temperatures. In lower temperatures, the highest frequencies are controlled by the nucleation criterion, $\nu_{\max} = \nu(l_{\max})$. In higher temperatures, maximum crystallization frequency $\nu_{\max}$ is higher than $\nu(l_{\max})$. Consequently, plates thinner than $l_{\max}$ are formed faster (Fig. 14). The $l(T; \nu_{\max})$ characteristic deviates from the $l_{\max}(T)$ and approaches the thermodynamic limit $l_{\min}(T)$ [see Eq. (16)]. For a fixed plate thickness, the frequency $\nu_{0k}^{spc}(l_k, T)$ decreases with increasing

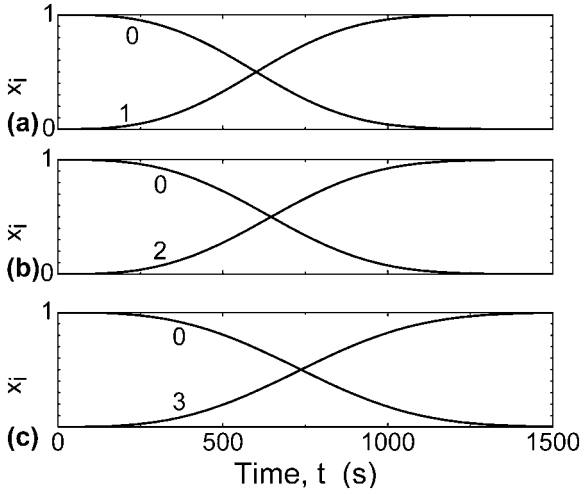


FIG. 20. Isothermal development of phase composition at 375 K in isolated two phase systems in case of $l_k > l(\nu_{\max})$. 0—amorphous phase, (a) Transition $0 \rightarrow 1$ ($l_1 = 1.23 \times 10^{-6}$ cm), (b) Transition $0 \rightarrow 2$ ($l_2 = 1.32 \times 10^{-6}$ cm), (c) Transition $0 \rightarrow 3$ ($l_3 = 1.40 \times 10^{-6}$ cm).

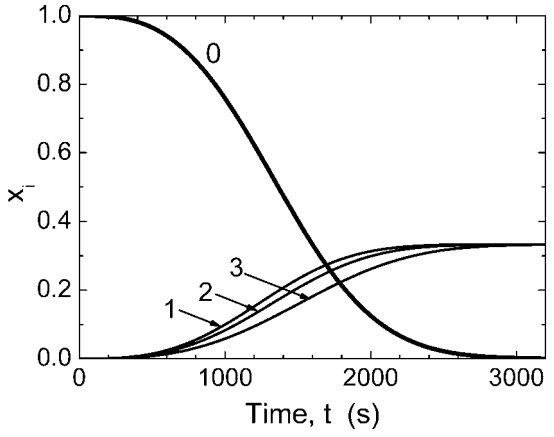


FIG. 21. Simultaneous isothermal development of phase composition at 375 K for a system containing three plate-like solids with different thicknesses $l_k > l(\nu_{\max})$. 0—amorphous phase, 1—crystals with $l_1 = 1.23 \times 10^{-6}$ cm, 2—$l_2 = 1.32 \times 10^{-6}$ cm, 3—$l_3 = 1.40 \times 10^{-6}$ cm, amorphous fractions assumed $f_1 = f_2 = f_3 = 1/3$.

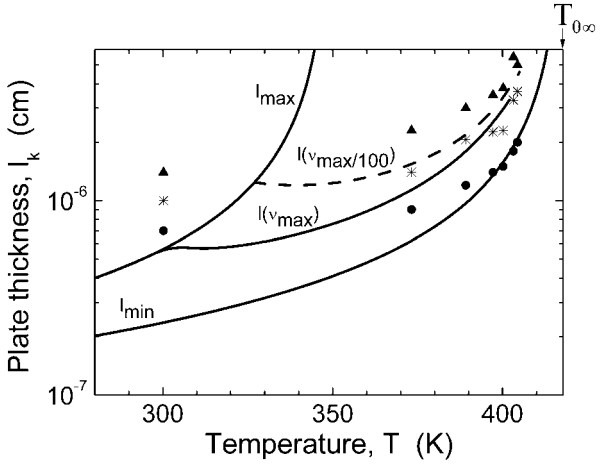


FIG. 22. Crystalline plate thickness versus temperature on the map of the plate-like crystallization model for linear polyethylene with parameters from Table II. Solid lines: computed $l_{\min}$, $l_{\max}$, $l(\nu_{\max})$. Dashed line: computed $l(\nu_{\max}/100)$ at frequency $\nu_{\max}/100$. Points: experimental data[22] (solid circles—minimum, stars—average, and solid triangles—maximum thickness).

https://doi.org/10.1557/jmr.2013.74 Published online by Cambridge University Press

TABLE II. Material characteristics for linear polyethylene.

Parameter	Characteristic	Value	Source
$T_{\infty 0}$ (K)	Melting temperature	417.8	12
$\Delta h_{\infty 0}$ (J/cm^3)	Heat of melting	280.0	12
E_D^{0k} (kJ/mol)	Activation energy in the melt	25.0	20
σ_e (J/cm^2)	Interface tension on plate surface	9.3×10^{-6}	12
σ_s (J/cm^2)	Interface tension on plate sides	1.41×10^{-6}	12
a_0^2 (cm^2)	Base area of the kinetic unit	18.9×10^{-16}	12

temperature [Fig. (15)]. Significant reduction of $\nu_{0k}^{spc}(l_k, T)$ is observed well below the melting temperature, T_{k0}.

The character of plate thickness effects described by the present model is consistent with experimental data on linear polyethylene.[22] Minimum, maximum, and average plate thicknesses increase with increasing crystallization temperature and tend to infinity in a temperature, $T_{\infty 0}$, characteristic of melting infinitely thick crystals. Figure 22 presents plate thickness as a function of temperature. Solid lines represent $l_{min}(T)$, $l_{max}(T)$, and $l[\nu_{max}(T)]$ calculated from the model [Eqs. (16) and (17)] with parameters collected in Table II. The dashed line represents thickness of plates characterized by $\nu = 0.01 \cdot \nu_{max}$ which can be treated as a practical limit of the observed distribution of plate thicknesses. Points represent experimental data of polyethylene plates' thickness taken from the paper of Voigt-Martin and Mandelkern.[22]

The calculated values of $l(\nu_{max})$ can be compared with average experimental thicknesses and $l(0.01 \cdot \nu_{max})$ with maximum thicknesses observed in the experiments.

It is evident that experimental data reasonably well fit the thickness range predicted by the model. Only in the low temperature ($T = 300$ K), three experimental points depart from the predicted range and lie above the l_{max} limit. It should be noted that these points appear in the range where crystallization is not controlled by the nucleation mechanism and are beyond the scope of the present model.

Phase composition developed in isothermal crystallization strongly depends on temperature and plate thickness. Two temperature regimes can be distinguished (Fig. 13). The low temperature region is characterized by overlapping terminal transition frequency, $\nu(l_{max})$, and maximum frequency, ν_{max}. In this range, thick crystals are formed faster than thin ones (Fig. 14). In the high temperature range, thick plates with thickness $l_{min} < l_k \leq l(\nu_{max})$ are created faster than thin ones, while the opposite behavior applies when plate thickness lies in the range $l(\nu_{max}) \leq l_k \leq l_{max}$ (Fig. 14). The above relations can be used to control plate structure of the material.

Development of crystallinity predicted by the present model in α-isotactic polypropylene at $T = 396$ K is compared with experimental data of Sajkiewicz et al.[8] Relative crystallinity $x(t)/x(t = \infty)$ is plotted versus time in Fig. 23. The plate thicknesses selected for the model computations are $l_1 = l[\nu_{max}(T = 396\ \text{K})]$, $l_2 = 1 - (\nu_{max/2})$, and $l_3 = l + (\nu_{max/2})l_1$ corresponds to maximum crystallization frequency, l_2 and l_3 are placed on both sides of the frequency distribution function $\nu(l, T)$ at $\nu = 1/2\nu_{max}$. To obtain good fit with experimental data, the material parameters are chosen from Table I, with $E_D^{0k} = 70$ kJ/mol and $\sigma_e = 6.23 \times 10^{-6}$ J/cm^2 (Ref. 21). The experimental data are reasonable well reproduced in Fig. 23 with the thicknesses of the crystal plates determined by the maximum frequency and the half-width of the frequency distribution.

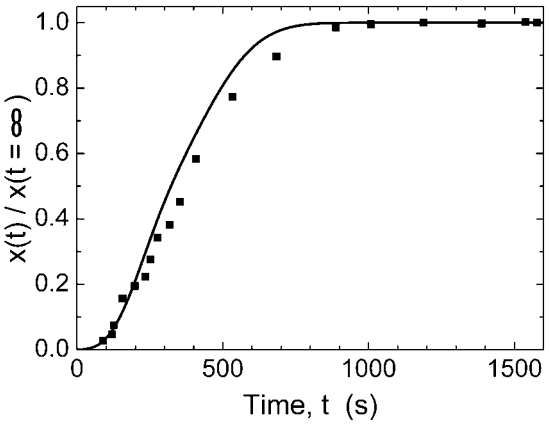


FIG. 23. Relative crystallinity versus time for α-polypropylene at 396 K. The line plot: computed from the model with the parameters from Table I with $E_D^{0k} = 70$ kJ/mol, $\sigma_e = 6.23 \times 10^{-6}$ J/cm^2 (Ref. 21), and $l_1 = 6.70 \times 10^{-7}$ cm, $l_2 = 5.49 \times 10^{-7}$ cm, $l_3 = 8.61 \times 10^{-7}$ cm. Points: experimental data for α-polypropylene.[8]

The model shows that higher temperatures lead to longer crystallization times when sporadic nucleation is involved. To speed up the transition, an addition of predetermined nuclei is suggested.[2,18]

ACKNOWLEDGMENT

The author acknowledges helpful discussions held with Professor A. Ziabicki and Professor L. Jarecki.

REFERENCES

1. A. Ziabicki and B. Misztal-Faraj: Modeling of phase transitions in three-phase polymorphic systems: Part I. Basic equations and example simulation. *J. Mater. Res.* **26**(13), 1586–1595 (2011).

https://doi.org/10.1557/jmr.2013.74 Published online by Cambridge University Press

2. B. Misztal-Faraj and A. Ziabicki: Modeling of phase transitions in three-phase polymorphic systems: Part II. Effects of material characteristics on transition rates. *J. Mater. Res.* **26**(13), 1596 (2011).
3. A.N. Kolmogorov: On statistical theory of metal crystallization. *Izv. Akad. Nauk SSSR, Ser. Math.* **3**, 355 (1937).
4. M. Avrami: Kinetics of phase change. I General theory. *J. Chem. Phys.* **7**, 1103 (1939).
5. M. Avrami: Kinetics of phase change. II Transformation-time relations for random distribution of nuclei. *J. Chem. Phys.* **8**, 212 (1940).
6. M. Avrami: Granulation, phase change, and microstructure. Kinetics of phase change. III. *J. Chem. Phys.* **9**, 177 (1941).
7. U.R. Evans: The laws of expanding circles and spheres in relation to the lateral growth of surface films and the grain-size of metals. *Trans. Faraday Soc.* **41**, 365 (1945).
8. P. Sajkiewicz, A. Gradys, A. Ziabicki, and B. Misztal-Faraj: On the metastability of β phase in isotactic polypropylene: Experiments and numerical simulation. *e-Polymers* **124**, 1–20 (2010).
9. A. Keller: A note on single crystals in polymers: Evidence of a folded-chain configuration. *Philos. Mag.* **2**, 1171 (1957).
10. J.D. Hoffman and J.I. Lauritzen, Jr.: Crystallization of bulk polymers with chain folding: Theory of growth of lamellar spherulites. *J. Res. Nat. Bur. Stand.* **65A**, 297 (1961).
11. J.D. Hoffman: Theoretical aspects of polymer crystallization with chain folds: Bulk polymers. *Soc. Plast. Eng. Trans.* **4**, 315 (1964).
12. J.D. Hoffman, G.T. Davis, and J.I. Lauritzen, Jr.: The rate of crystallization of linear polymers with chain folding, in *Treatise on Solid State Chemistry*, Vol. **3**, edited by N.B. Hannay (Plenum Press, New York, NY, 1976), pp. 497–614.
13. A. Ziabicki: Nucleation-controlled multiphase transitions. *J. Chem. Phys.* **123**, 174103 (2005).
14. D. Turnbull: Formation of crystal nuclei in liquid metals. *J. Appl. Phys.* **21**, 1022 (1950).
15. J. Frenkel: *Kinetic Theory of Liquids* (Oxford University Press, London, 1946).
16. Y.B. Zeldovich: Theory of formation of a new phase: Cavitation. *Acta Phys.Chim. USSR* **18**, 1 (1943).
17. F.C. Frank and M. Tosi: On the theory of polymer crystallization. *Proc. R. Soc. London, Ser. A* **263**, 323 (1961).
18. B. Misztal-Faraj and A. Ziabicki: Effects of predetermined nuclei and limited transformation on polymorphic crystallization in a model polymer. *J. Appl. Polym. Sci.* **125**, 4243 (2011).
19. B. Monasse and J.M. Haudin: Growth transition and morphology change in polypropylene. *Colloid Polym. Sci.* **263**, 822 (1985).
20. D.W. Van Krevelen: *Properties of polymers* (Elsevier, Amsterdam, 2000), pp. 469, 597.
21. J.E. Mark: *Physical Properties of Polymers Handbook* (American Institute of Physics, Woodbury, NY, 1996), p. 424.
22. I.G. Voigt-Martin and L. Mandelkern: A quantitative electron-microscopic study of a linear polyethylene fraction crystallized at different temperature. *J. Polym. Sci.* **19**, 1769–1790 (1981).

https://doi.org/10.1557/jmr.2013.74 Published online by Cambridge University Press